

Isolation of magnetically tagged cancer cells through an integrated magnetofluidic device

Qi Ying Wong¹ · Ning Liu¹ · Cheng-Gee Koh² · Hoi-Yeung Li² · Wen Siang Lew¹ 

Received: 13 July 2016 / Accepted: 13 September 2016 / Published online: 24 September 2016
© Springer-Verlag Berlin Heidelberg 2016

Abstract Circulating tumour cells (CTC) in the bloodstream has been implicated in cancer metastasis. Efficient removal of CTC could potentially be an effective therapeutic measure against cancer metastasis. In this study, the hydrodynamic focusing flow in microfluidic channels ($Re \ll 1$) was considered together with the magnetophoretic force. The localised magnetic field was achieved through a passivated current-carrying multilayered microstripline, where the generated field gradient was used to attract the magnetic beads to the desired outlet. The experimental results show that the device is capable of isolating purely magnetic beads with an efficiency of 91 % while isolation efficiency of the magnetically tagged HeLa cervical cancer cells from cell suspension yielded an isolation efficiency of 79 %.

1 Introduction

Cancer has claimed many lives leading to increasing efforts in cancer diagnostics and anti-cancer strategy research. Cancer cells can spread to secondary sites via the bloodstream in the form of circulating tumour cells (CTC) (Bacac and Stamenkovic 2008) in a process known as metastasis. Numerous research programmes aim to identify the processes involved in metastasis. However, methods to

effectively remove CTC from the circulatory system are limited (Chiang and Massagué 2008). As such, the detection and eradication of CTC from the bloodstream are important in complementary anti-cancer therapeutic strategy in which magnetic particles are utilised. Magnetic particles (Nguyen et al. 2006) can be manipulated remotely by magnetic forces induced by either a permanent magnet or an electromagnet placed in close proximity. There are several biological-related applications for an integrated magnetic Lab-on-Chip (LOC) system which includes cancer cell destruction (Kim et al. 2010), virus detection (Lee et al. 2008), immunoassays (Lim and Zhang 2007), protein analysis (Choi et al. 2002) and cell separation (Hejazian et al. 2015; Inglis et al. 2004). Magnetic beads have become an essential part of these magnetic devices as they can be easily functionalised by tagging with desired biomolecules such as DNA, antibodies, proteins and cells (Gijs et al. 2009; Pamme 2006). After which, they can be manipulated and separated (Choi et al. 2001; Deng et al. 2002) based on the behaviour of the magnetic fields applied. Magnetofluidic devices utilising both fluid flow and magnetic fields have detected and isolated magnetically labelled CTC cells within the bloodstream (Dolgin 2011; Nagrath et al. 2007; Pamme and Wilhelm 2006; Tan et al. 2009). This magnetic manipulation utilises external magnets that sort and detect magnetically tagged molecules and cells and have become a well-known technique in biotechnology (Roath et al. 1990; Whitesides et al. 1983). Magnetophoresis involves the utilisation of high field gradients to drive magnetic particles along the gradient line, (Nguyen 2012) which is the concept used in the implementation of permanent magnets in magnetic separation systems (Haik et al. 1999; Hatch and Stelter 2001; Zborowski et al. 1999). High field gradients drive the separation of magnetic particles, and this has been also reported extensively (Gijs et al. 2009; Melville et al.

✉ Wen Siang Lew
wensiang@ntu.edu.sg

¹ School of Physical and Mathematical Sciences,
Nanyang Technological University, 21 Nanyang Link,
Singapore 637371, Singapore

² School of Biological Sciences, Nanyang Technological
University, 60 Nanyang Drive, Singapore 637551, Singapore

1975, 1982; Miltenyi et al. 1990; Oberteuffer 1973; Richards et al. 1996). Some reported the use of ferromagnetic structures with various geometries (Kang and Park 2007; Smistrup et al. 2005; Yellen et al. 2007) to generate a field gradient large enough to direct a stream of magnetic particles towards the desired outlet. These methods are widely investigated; however, an alternate method was to use current conducting electromagnets in the form of microcoils (Song et al. 2009) and microstrips (Derec et al. 2009; Jiang et al. 2006; Joung et al. 2000; Kong et al. 2011) to generate a magnetic field gradient. Few have used such an approach to fabricate an integrated magnetofluidic device with a tunable current-generated field to isolate magnetic particles. The tunable nature of the field allows for magnetic particles to flow freely without causing agglomeration in the microchannel obstructing the flow of the fluid, which happens when permanent magnets are used. Isolation of particles using an integrated tunable magnetic field is scarcely explored.

In this study, an integrated portable magnetofluidic microchip was designed to isolate HeLa cells that are tagged with magnetic microparticles. Under the influence of an applied magnetic field generated by the current-carrying microstripline, the HeLa cells are expected to be driven to the desired outlet. The movement of the cells is controlled by the flow dynamics of the microchannel as well as the strength of the applied magnetic field.

2 Theory and simulation

In the theory of fluids at the microfluidic level, it is known that the mass transport within the fluid is dominated by the viscous effects, while the inertial effects are negligible in comparison due to the fundamental property of the nature of fluid flow, Reynold's number, Re . In a microfluidic device, the $Re \ll 1$, which linearises the Navier–Stokes equation to the Stokes drag equation given by

$$F_{\text{drag}} = \frac{1}{8} C_D \pi A \rho_{\text{fluid}} v^2,$$

where C_D is given as the dimensionless drag coefficient, A is the cross-sectional area of the object, ρ_{fluid} is the density of the fluid, and v is the speed of the object relative to the fluid.

In magnetic sortation theory, the magnetic force is a volume-based force and at the microscale, the use of a permanent magnet is not suitable for particle isolation as it causes particles to be trapped and cannot be sophisticatedly removed and controlled accurately. As such, electrically controlled magnetic fields are preferred as it allows the field to be tuned accordingly. The deflection of the magnetic particles v_{defl} (m/s) can be described as the vector

sum of the magnetically induced flow velocity of the particle v_{mag} and the velocity due to the hydrodynamic flow v_{hyd} : (Pamme and Manz 2004)

$$v_{\text{defl}} = v_{\text{mag}} + v_{\text{hyd}},$$

The magnetically induced flow, v_{mag} , is the ratio of the magnetic force, \mathbf{F}_{mag} (N), exerted on the particle by the magnetic field to the viscous drag force:

$$v_{\text{mag}} = \frac{F_{\text{mag}}}{F_{\text{drag}}} = \frac{F_{\text{mag}}}{6\pi\eta r},$$

The magnetophoretic force on a superparamagnetic bead can be expressed as and utilising the vector calculus identity $\nabla(\mathbf{B} \cdot \mathbf{B})B = 2\mathbf{B} \times (\nabla \times \mathbf{B}) + 2(\mathbf{B} \cdot \nabla)B = 2(\mathbf{B} \cdot \nabla)B$,

$$F_{\text{mag}} = \frac{V_{\text{bead}}\Delta\chi}{\mu_0} (\mathbf{B} \cdot \nabla)B = \frac{V_{\text{bead}}\Delta\chi}{2\mu_0} \nabla B^2,$$

where $\Delta\chi$ is the difference between the magnetic susceptibilities of the bead and the fluid and V_{bead} is the volume of the bead.

Magnetostatic and flow dynamics simulations are performed using COMSOL Multiphysics program. The magnetic simulation results are shown in Fig. 1. Through the employment of a current through the double microstripline, magnetic flux is generated around it. The magnitude of magnetic field gradient in the y component plays the most significant role in the deflection of the magnetic particles, while the x and z components also increase the overall magnetic flux density of the device. The average magnetic flux generated by the microstripline when 0.9A current is passing through can be determined by $B_{\text{total}} = \sqrt{B_x^2 + B_y^2 + B_z^2}$ and $B_{\text{total}} = 347G$ which according to the particle flow simulations will be sufficient to deflect the magnetic particles. The magnetic simulations are consistent with Biot–Savart's Law ($B \propto I$) as there is a proportionate relation between the magnitude of the magnetic flux and current. The magnetic particles are then attracted to the current-carrying microstripline given by the magnetophoretic force equation governed by $F_{\text{mag}} = \frac{V_{\text{bead}}\Delta\chi}{2\mu_0} \nabla B^2$. The average magnetophoretic force from a 0.9A field generating microstripline was determined to be (7.5 ± 0.2) pN using the mentioned magnetophoretic force equation inputted into MATLAB.

Thermal characterisation of the device was done by simulation of joule heating in the microstripline. The average surface temperature was determined after 5 min of passing current through the double microstripline. This is done in order to estimate the likely real time temperature increase in the surface of the magnetofluidic chip. Simulations were performed for different current values from 0.4 to 0.9 A with intervals of 0.1 A with the initial temperature conditions set as 25 °C and heat transfer coefficient of copper with water interface as 13.1 W/m²K, and the surface emissivity of copper is 0.87. Simulation results

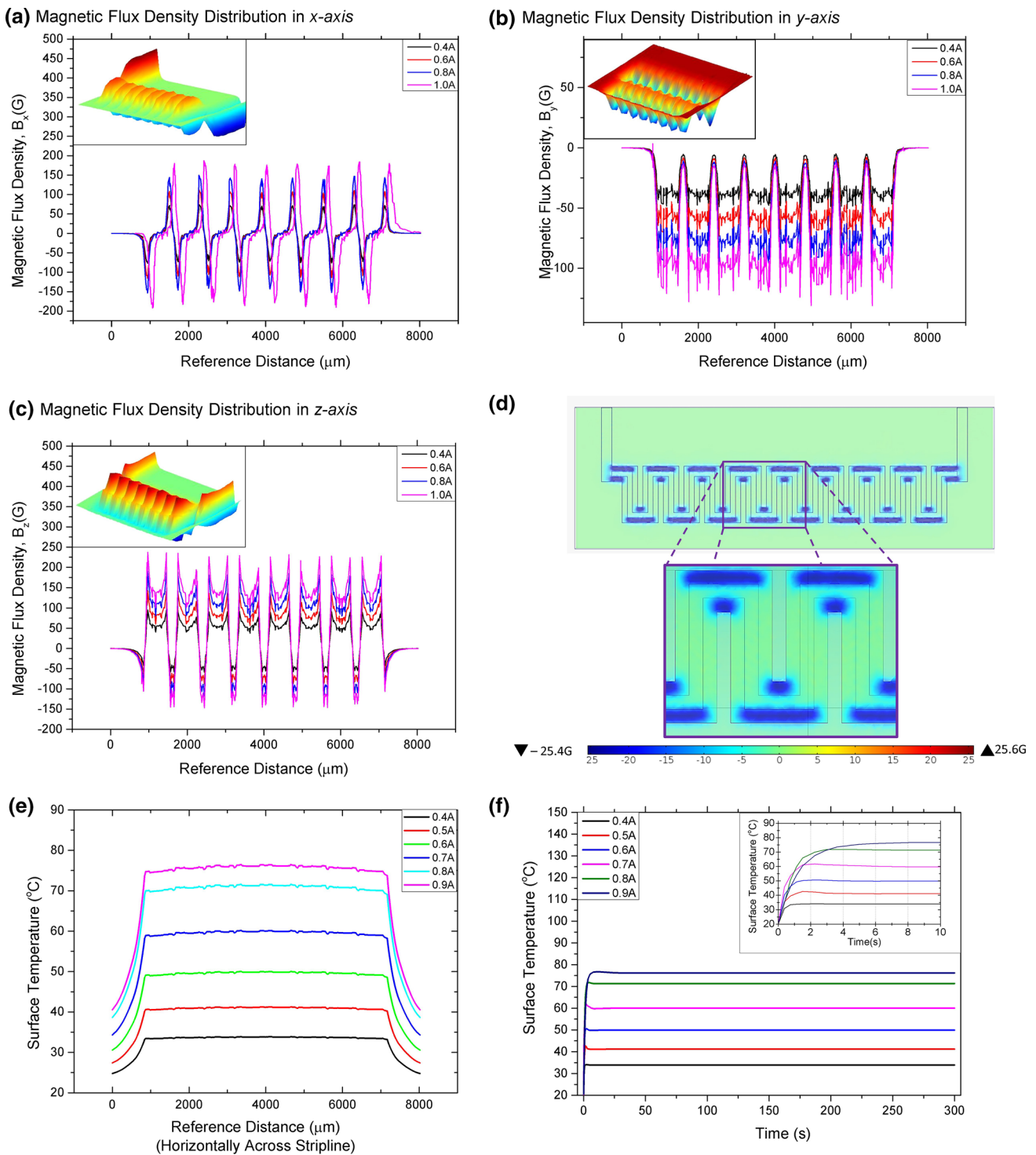


Fig. 1 a–c Magnetic flux density distribution in the x , y and z components for the current values $0.4 \text{ A} \leq I \leq 1.0 \text{ A}$ along a reference line of measurement at the centre of the microstripline. **d** Magnetic field gradient distribution of the y component in the double

microstripline structure with current at 0.4 A. **e** Surface temperature distribution along the microstripline for current values ranging $0.4 \text{ A} \leq I \leq 0.9 \text{ A}$. **f** Temperature change across the microstripline after a period of 5 min for current values ranging $0.4 \text{ A} \leq I \leq 0.9 \text{ A}$

have affirmed that joule heating will not be an issue, and this is confirmed experimentally. External cooling was not required. However, in order to ensure the complete

viability of cells, external cooling was implemented for the experiment conducted with cells. External cooling was done by incorporating a Peltier dielectric chip below

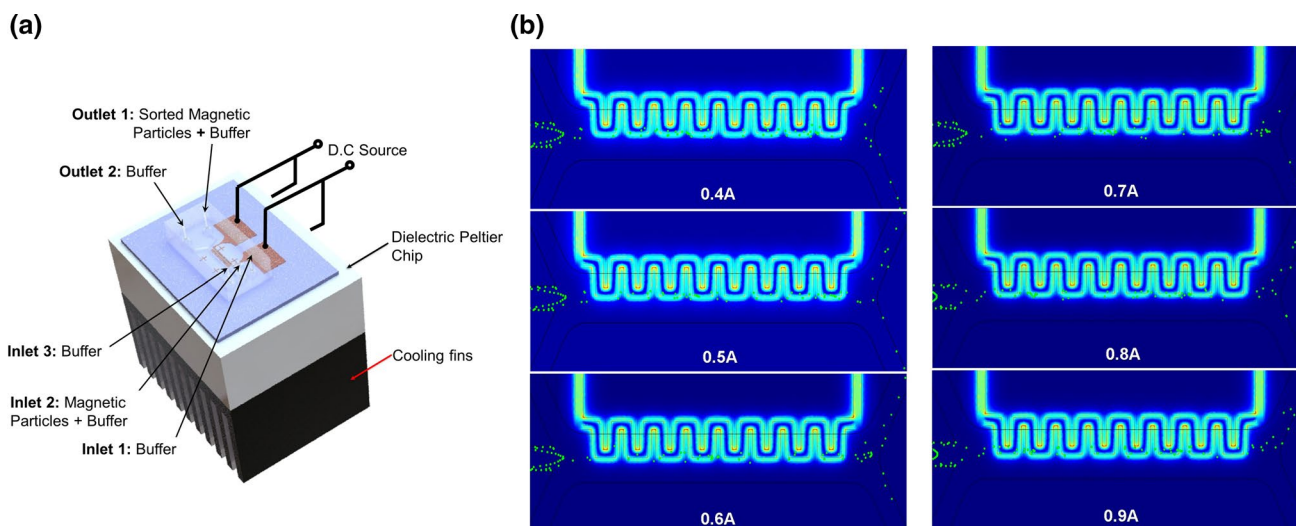


Fig. 2 **a** Schematic of experimental setup of the magnetofluidic device on top of a dielectric Peltier cooling chip fitted with cooling fins for cooling down of the chip. **b** Simulations of magnetic particle flow in a magnetofluidic microchip for current values ranging

$0.4 \text{ A} \leq I \leq 0.9 \text{ A}$, partial deflection occurs at 0.6 A, and complete deflection occurs at 0.9 A. The flow is governed by the Navier–Stokes equation, and the beads flow is forced to the central line using the hydrodynamic focusing approach

the magnetofluidic chip to cool the chip as shown by the schematic of the experimental setup, as shown in Fig. 2. In order to determine the effect of heating on the HeLa cells, cell viability for current values of 0.4, 0.6 and 0.9 A was determined as 92.2, 89.6 and 87.2 %, respectively. Additionally, 100 % cell viability was attained when cooling was implemented.

In the fluid dynamics simulation, the laminar flow profile from three inputs is simulated. The flow rates of the three inlets are varied so as to focus the middle streamline close to the centre of the microchannel, and this is governed by the Navier–Stokes equation and the continuity equation. By introducing particles in the simulation, hydrodynamic focusing is seen as shown in Fig. 2. Hydrodynamic focusing occurs when flow streams with different flow rates come into contact with each other (Chang et al. 2007; Jahn et al. 2004; Morgan et al. 2003; Simonnet and Groisman 2005). Upon the application of a magnetic field, the profile of the magnetic particle stream will deviate to the outlet where the magnetic field gradient points towards. The entire magnetofluidic device was simulated, and significant deflection of the magnetic beads was observed at 0.6 A with complete deflection of the magnetic beads occurring at an input current of 0.9 A. From the simulations and theoretical understanding, the particles are influenced by two forces, the drag force from the fluid and magnetic attraction force from the magnet. The gravitational effect is neglected because it is only acting on z direction. The simulation of particle separation is shown in Fig. 2.

3 Experimental methods

3.1 Fabrication of device

The integration process involved multiple optical lithography steps (Beebe et al. 2002). A double square meandering structure was fabricated for device fabrication. A square meandering structure (Ramadan et al. 2006b) shows promising high efficiency in the magnetic actuation process (Kong et al. 2011). A multilayered microstripline structure (Maloratsky 2000) is integrated into the device for magnetic field generation. Thermally grown silicon dioxide (300 nm) silicon wafer is used as the substrate for the microstripline fabrication. A thick positive resist AZ9260 imaging resist (AZ electronics) and LOR-3B (Microchem) was spun coated onto the wafer. In order to ensure clean lift-off, ion milling was done to create a trench to enhance adhesion. A double square meandering patterned structure is preferred over the single meandering structure as it has higher efficiency in magnetic actuation determined through simulation.

A metallic multilayer comprising of Cr(3 nm)/NiFe/SiO₂/Cu/Cr structure is deposited on the resist-patterned wafer using electron-beam evaporation techniques. The Cr layer serves as a seed layer to enhance the bonding of the following conduction layer. The SiO₂ layer between NiFe and Cu was used as a passivation layer which decreases the total resistance of the structure by separating the permalloy and the conducting Cu layer, and other alternatives such as photoresist could be used as the dielectric passivation

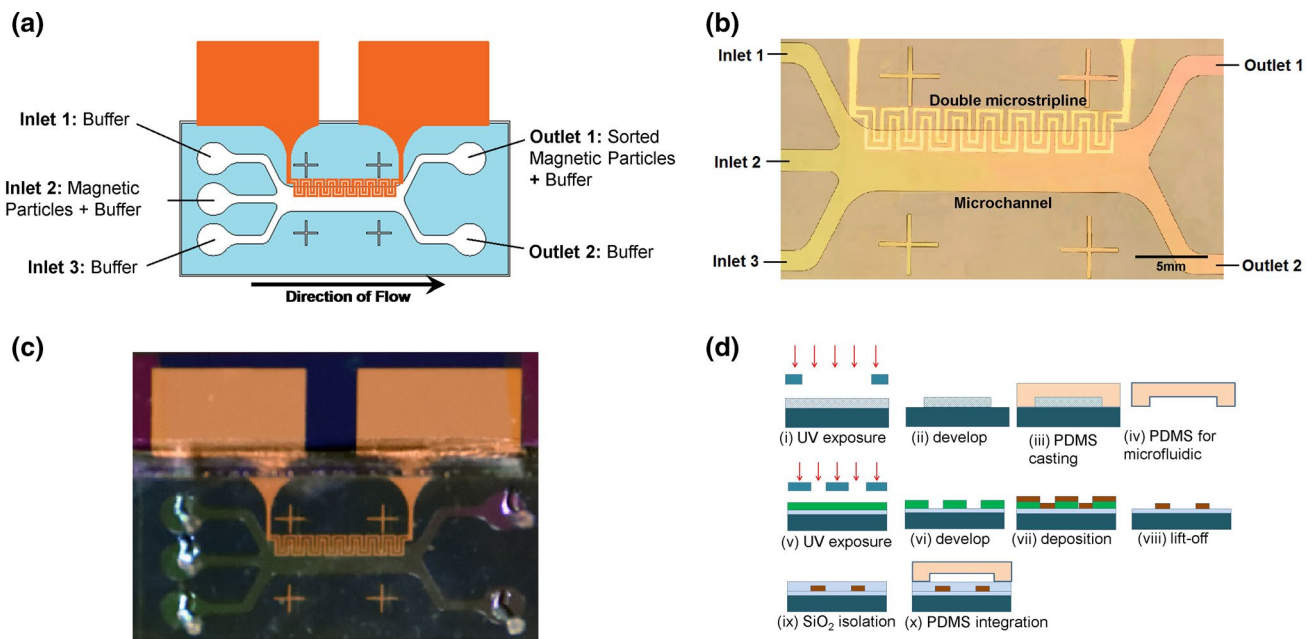


Fig. 3 **a** Design schematic of the magnetofluidic device indicating the flow of magnetic particles, **b** optical micrograph of the magnetofluidic device and **c** a prototype of the magnetofluidic microchip. **d** Overview of the device fabrication process. Processes (i)–(iv) show the step-by-step fabrication of PDMS microchannel. Processes (v)–

(viii) show the standard photolithography and physical vapour deposition techniques that are used to fabricate the microstripline. Processes (ix)–(x) show the integration of the microfluidic and the microstripline

(Song et al. 2009), but in this case, SiO₂ was preferred. The Cu layer serves as the main conduction layer for the generation of the magnetic field when an electric current flows through it. The ferromagnetic permalloy (NiFe) was used to concentrate the path of the flux lines by creating a new low reluctance path, hence increasing the magnetic flux gradient and enhances the actuation of magnetic particles. The final Cr layer serves as a protection capping layer to prevent the process of oxidation to the conducting Cu layer.

After the microstripline structural deposition, a SiO₂ insulating or passivation layer is deposited using the electron-beam evaporation technique. This allows the isolation of the metallic microstripline structure from the liquid flow in the microchannel. SiO₂ was used to effectively insulate the microstripline from the liquid. The maximum thickness of the passivation layer was confined to below 300 nm in order to maintain an effective magnetic field experienced by the magnetic particles. The optimised thickness of the passivation layer was determined to be 100 nm so that passivation and good bonding of the PDMS microfluidic channel could be effectively achieved.

The microfluidic channel (Chen et al. 2013; Ramadan et al. 2006a; Whitesides et al. 2001) was fabricated using conventional soft lithography technique (Fiorini and Chiu 2005; Qin et al. 1998; Whitesides et al. 2001). This was carried out by casting PDMS (Sylgard 184) against a master patterned with a thick SU8-3035 negative resist. Figure 3

summarises the fabrication processes for the microchannel and microstripline. Upon successful development of the essential fabrication techniques and experimental optimisation of the microfluidic system and microstriplines, they were integrated into one compact system.

Figure 3 illustrates the integrated magnetofluidic microchip which consists of the double microstripline and microchannel with three inlets and two outlets incorporated into an integrated magnetofluidic device as well as the detailed fabrication process of the magnetofluidic device. The overall dimension of the fabricated device is 35 mm × 35 mm.

4 Results and discussions

Glycerol mixture (glycerol/water = 1:1) was first used to simulate the viscosity of blood. Before the application of the magnetic field, the flow rate at the inputs is adjusted so as to confine the particle flow at a position just exactly above the centre line of the sorting chamber. Hydrodynamic focusing happens as predicted by simulation results. Hydrodynamic focusing is to ensure that without the application of a field, the particle stream will always flow into outlet 2. In addition, the particle stream is close to the centre of the microchannel, and the magnetic field strength needed to coerce the particles to flow into outlet 1 is minimised. In the presence of a gradient magnetic field, the

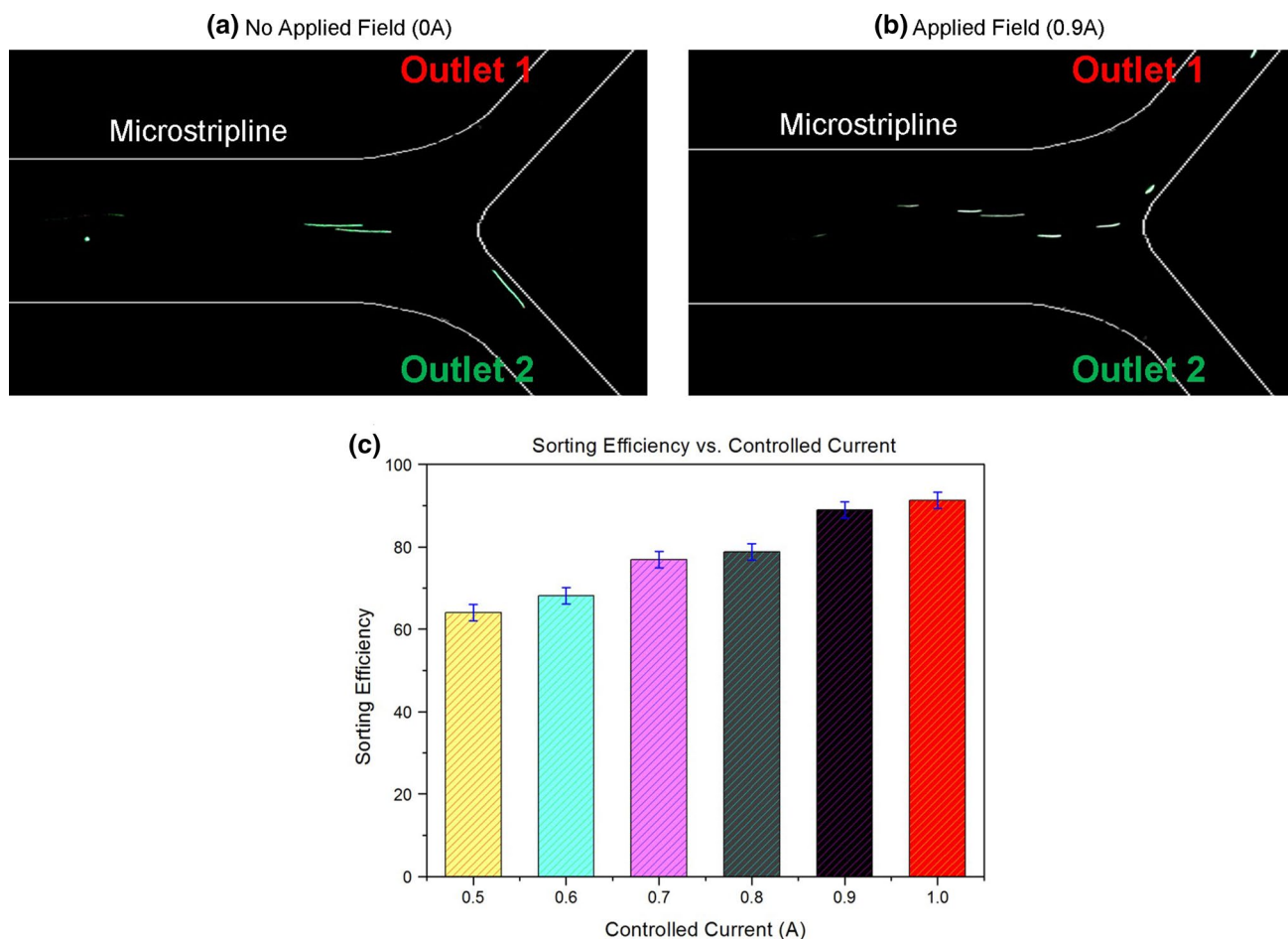


Fig. 4 Magnetic particles sorting in glycerol mixture. **a** When no current was applied, the magnetic particles flow to Outlet 2 and upon the activation of a minimum current of 0.5 A, deflection starts to

show and **b** at 1.0 A, 91 % of the particles are deflected. **c** Sorting efficiency relationship with a controlled current

magnetic particles will change their path of flow and switch to another streamline closer to the field-generating double microstripline. Thus, by gradually changing the flow path of the magnetic particles the device is able to direct the magnetic particles to outlet 1. Figure 4 shows the result of sorting of the magnetic beads going through Outlet 1. This result is repeated with increasing current values from 0.5 to 1.0 A. The minimum current of 0.5 A would have been sufficient to generate a magnetic field to deflect the microbeads.

The isolation efficiency is calculated by $\frac{O_D}{O_D + O_N} \times 100\%$, where O_D is the number of deflected particles and O_N is the number of non-deflected particles. This was then calculated by post-processing the images. As control at zero current, the stream was adjusted to just flow close to Outlet 2, and when a current is applied, the beads will then be deflected to Outlet 1 due to the presence of the magnetic field. By increasing the current, the magnetic field gradient generated by the microstripline increased. As such, the isolation

efficiency increases. At 1.0 A current, the magnetic field generated is sufficient to cause an isolation efficiency of 91 %. Upon proving the concept of deflection using the magnetofluidic device, this similar principle is brought to the separation of magnetic particle tagged HeLa cells.

4.1 Magnetic particle tagging of HeLa cells

Mouse monoclonal EpCAM (C-1) antibodies [sc-25308] were chosen for the detection and isolation of cells in this study. The monoclonal antibody recognises the EpCAM antigen that is expressed on the HeLa cells. 2 mg of COMPEL™ 8- μ m magnetic beads (with green fluorescence) is washed with 1 ml of 2-(N-Morpholino)ethanesulfonic acid (MES) [0.1 M, pH 5] buffer for about 3 times. The magnetic particles are isolated by a magnet and washed with PBS. The washed particles are activated by suspending them in MES buffer containing 10 mg of 1-ethyl-3-(3-dimethylaminopropyl) carbodiimide (EDC) and rolled for

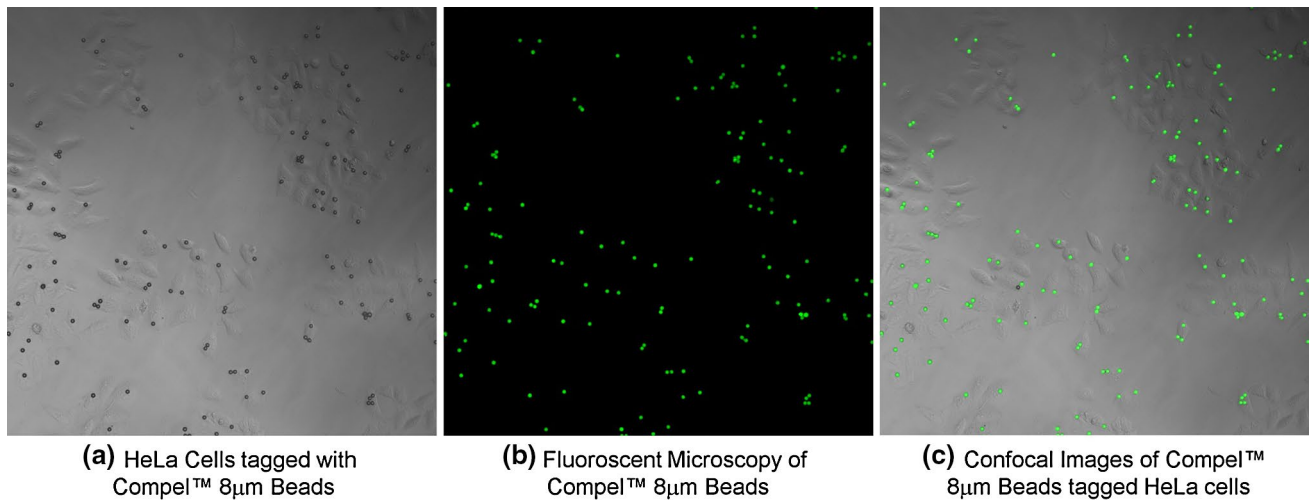


Fig. 5 High binding efficiency of the EpCAM (C-1) antibodies-conjugated COMPEL™ 8-μm magnetic beads to HeLa cells was observed on an optical microscope, **b** fluorescent microscopy, **c** confocal images. Multiple magnetic beads could be found attached to the cell

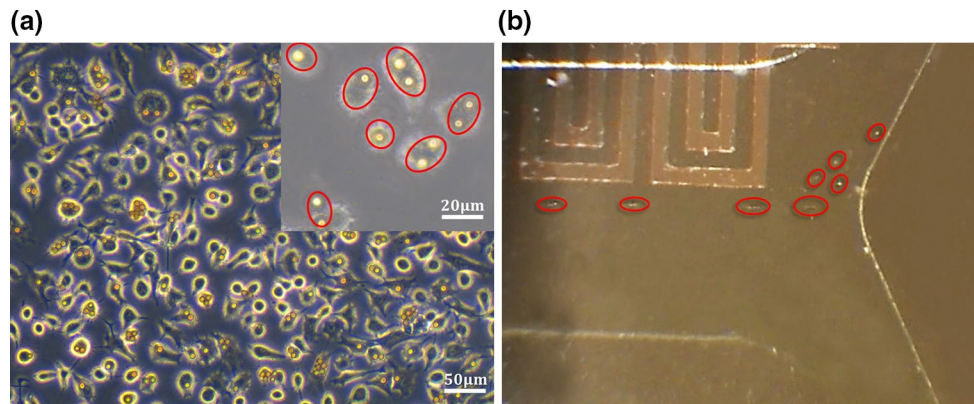


Fig. 6 **a** Sorting of HeLa cancer cells using EpCAM (C-1) antibodies-conjugated COMPEL™ 8-μm magnetic beads at Outlet 1 when 0.9 A current was applied to the microstripline to generate the magnetic field. *Red circles* indicate the tagged cells that are in Outlet 2. A sorting efficiency of $79 \pm 1\%$ is consistently obtained; this effi-

ciency is calculated based on the collected cell count at outlets 1 and 2 after 30 min. **b** Optical microscope image of the deflection of the tagged HeLa cancer cells in the microchannel when 0.9 A current was applied (colour figure online)

30 min at room temperature. The monoclonal antibodies are then added to the activated magnetic particles and incubated on a rocker overnight at room temperature. Finally, the mouse monoclonal EpCAM (C-1) antibodies-conjugated COMPEL™ 8-μm magnetic beads were resuspended in 100 μL PBS. 1×10^6 HeLa cells were re-suspended in 0.9 ml of completed DMEM culture medium. 100 μL of anti-EpCAM antibody-conjugated COMPEL™ 8-μm magnetic beads in DMEM culture medium was added to the 0.9 ml cell suspension and incubated at 37°C for 60 min. Binding of the anti-EpCAM antibody-conjugated COMPEL™ 8-μm magnetic beads to HeLa cells was verified using a fluorescence microscope. Figure 5 shows the efficient tagging of the HeLa cells with the magnetic beads.

4.2 Sorting of magnetically tagged HeLa cells

The mixture was then pumped into the sorting chamber with a controlled flow rate 1 μl/min that met the hydrodynamic focusing requirement similar to the magnetic bead only experiment. Video footages were taken at the centre of the dialyzer where magnetic field was applied. The strength of the magnetic field was adjusted by fine-tuning to the optimum field with current provided to the microstripline at 1.0 A. As a control, zero current was applied. Sorting was done in a process similar to the magnetic bead only experiment. The cells were then counted in Outlet 1 and Outlet 2 at the end of the experiment. The experiment was repeated and the average isolation efficiency for sorting the EpCAM

(C-1) antibodies-conjugated COMPEL™ 8- μm magnetically tagged HeLa cells were sorted into Outlet 1 is 79 %. The counting of the tagged cells was repeated, and consistent results within ± 1 % deviation were seen. Figure 6 illustrates the optical microscope image of the isolated HeLa cells in the sorted outlet and the sorting of the HeLa cells in the microchannel.

5 Conclusions

In conclusion, the fabricated double meandered microstrip-line microfluidic device is capable of sorting magnetic particles tagged HeLa cells with isolation efficiency of 79 %. The overall sorting efficiency is governed by the binding affinity and the number of EpCAM (C-1) antibodies-conjugated COMPEL™ 8- μm magnetic beads to HeLa cells. This study demonstrates the capability of the integrated magnetofluidic chip in isolating cells, and its capability is applicable to other types of cancer cells, thus serving as a potential application of such a device in anti-cancer treatment strategy through the detection and removal of CTC cells in the bloodstream.

Acknowledgments This work was supported by the Singapore National Research Foundation, Prime Minister's Office, under a Competitive Research Programme (Non-volatile Magnetic Logic and Memory Integrated Circuit Devices, NRF-CRP9-2011-01). WSL is a member of the Singapore Spintronics Consortium (SG-SPIN).

References

- Bacac M, Stamenkovic I (2008) Metastatic cancer cell. *Annu Rev Pathmechdis Mech Dis* 3:221–247
- Beebe DJ, Mensing GA, Walker GM (2002) Physics and applications of microfluidics in biology. *Annu Rev Biomed Eng* 4:261–286
- Chang C-C, Huang Z-X, Yang R-J (2007) Three-dimensional hydrodynamic focusing in two-layer polydimethylsiloxane (PDMS) microchannels. *J Micromech Microeng* 17:1479
- Chen J, Chen D, Yuan T, Xie Y, Chen X (2013) A microfluidic chip for direct and rapid trapping of white blood cells from whole blood. *Biomicrofluidics* 7:034106
- Chiang AC, Massagué J (2008) Molecular basis of metastasis. *N Engl J Med* 359:2814–2823
- Choi J-W, Liakopoulos TM, Ahn CH (2001) An on-chip magnetic bead separator using spiral electromagnets with semi-encapsulated permalloy. *Biosens Bioelectron* 16:409–416. doi:10.1016/S0956-5663(01)00154-3
- Choi J-W et al (2002) An integrated microfluidic biochemical detection system for protein analysis with magnetic bead-based sampling capabilities. *Lab Chip* 2:27–30
- Deng T, Prentiss M, Whitesides GM (2002) Fabrication of magnetic microfiltration systems using soft lithography. *Appl Phys Lett* 80:461–463
- Derec C, Wilhelm C, Servais J, Bacri J-C (2009) Local control of magnetic objects in microfluidic channels. *Microfluid Nanofluid* 8:123–130. doi:10.1007/s10404-009-0486-6
- Dolgin E (2011) New technologies aim to take cancer out of circulation. *Nat Med* 17(3):266. doi:10.1038/nm0311-266
- Fiorini GS, Chiu DT (2005) Disposable microfluidic devices: fabrication, function, and application. *Biotechniques* 38:429–446
- Gijjs MA, Lacharme F, Lehmann U (2009) Microfluidic applications of magnetic particles for biological analysis and catalysis. *Chem Rev* 110:1518–1563
- Haik Y, Pai V, Chen C-J (1999) Development of magnetic device for cell separation. *J Magn Magn Mater* 194:254–261. doi:10.1016/S0304-8853(98)00559-9
- Hatch GP, Stelter RE (2001) Magnetic design considerations for devices and particles used for biological high-gradient magnetic separation (HGMS) systems. *J Magn Magn Mater* 225:262–276. doi:10.1016/S0304-8853(00)01250-6
- Hejazian M, Li W, Nguyen N-T (2015) Lab on a chip for continuous-flow magnetic cell separation. *Lab Chip* 15:959–970. doi:10.1039/C4LC01422G
- Inglis DW, Riehn R, Austin RH, Sturm JC (2004) Continuous microfluidic immunomagnetic cell separation. *Appl Phys Lett* 85:5093–5095. doi:10.1063/1.1823015
- Jahn A, Vreeland WN, Gaitan M, Locascio LE (2004) Controlled vesicle self-assembly in microfluidic channels with hydrodynamic focusing. *J Am Chem Soc* 126:2674–2675
- Jiang Z, Llandro J, Mitrelias T, Bland J (2006) An integrated microfluidic cell for detection, manipulation, and sorting of single micron-sized magnetic beads. *J Appl Phys* 99:08S105
- Joung J, Shen J, Grodzinski P (2000) Micropumps based on alternating high-gradient magnetic fields. *IEEE Trans Magn* 36:2012–2014
- Kang JH, Park JK (2007) Magnetophoretic continuous purification of single-walled carbon nanotubes from catalytic impurities in a microfluidic device. *Small* 3:1784–1791
- Kim D-H, Rozhkova EA, Ulasov IV, Bader SD, Rajh T, Lesniak MS, Novosad V (2010) Biofunctionalized magnetic-vortex microdiscs for targeted cancer-cell destruction. *Nat Mater* 9:165–171. <http://www.nature.com/nmat/journal/v9/n2/abs/nmat2591.html#supplementary-information>
- Kong TF, Sugiarto HS, Liew HF, Wang X, Lew WS, Nguyen N-T, Chen Y (2011) An efficient microfluidic sorter: implementation of double meandering micro striplines for magnetic particles switching. *Microfluid Nanofluid* 10:1069–1078
- Lee W-C, Lien K-Y, Lee G-B, Lei H-Y (2008) An integrated microfluidic system using magnetic beads for virus detection. *Diagn Microbiol Infect Dis* 60:51–58. doi:10.1016/j.diagmicrobio.2007.07.010
- Lim CT, Zhang Y (2007) Bead-based microfluidic immunoassays: the next generation. *Biosens Bioelectron* 22:1197–1204. doi:10.1016/j.bios.2006.06.005
- Maloratsky LG (2000) Reviewing the basics of microstrip. *Microw RF* 39:79–88
- Melville D, Paul F, Roath S (1975) High gradient magnetic separation of red cells from whole blood. *IEEE Trans Magn* 11:1701–1704. doi:10.1109/TMAG.1975.1058970
- Melville D, Paul F, Roath S (1982) Fractionation of blood components using high gradient magnetic separation. *IEEE Trans Magn* 18:1680–1685. doi:10.1109/TMAG.1982.1062171
- Miltenyi S, Müller W, Weichel W, Radbruch A (1990) High gradient magnetic cell separation with MACS. *Cytometry* 11:231–238. doi:10.1002/cyto.990110203
- Morgan H, Holmes D, Green NG (2003) 3D focusing of nanoparticles in microfluidic channels. In: *IEE proceedings-nanobiotechnology*, vol 2. IET, pp 76–81
- Nagrath S et al (2007) Isolation of rare circulating tumour cells in cancer patients by microchip technology. *Nature* 450:1235–1239
- Nguyen N-T (2012) Micro-magnetofluidics: interactions between magnetism and fluid flow on the microscale. *Microfluid Nanofluid* 12:1–16. doi:10.1007/s10404-011-0903-5

- Nguyen N-T, Ng KM, Huang X (2006) Manipulation of ferrofluid droplets using planar coils. *Appl Phys Lett* 89:052509. doi:[10.1063/1.2335403](https://doi.org/10.1063/1.2335403)
- Oberteuffer J (1973) High gradient magnetic separation. *IEEE Trans Magn* 9:303–306. doi:[10.1109/TMAG.1973.1067673](https://doi.org/10.1109/TMAG.1973.1067673)
- Pamme N (2006) Magnetism and microfluidics. *Lab Chip* 6:24–38. doi:[10.1039/B513005K](https://doi.org/10.1039/B513005K)
- Pamme N, Manz A (2004) On-chip free-flow magnetophoresis: continuous flow separation of magnetic particles and agglomerates. *Anal Chem* 76:7250–7256
- Pamme N, Wilhelm C (2006) Continuous sorting of magnetic cells via on-chip free-flow magnetophoresis. *Lab Chip* 6:974–980. doi:[10.1039/B604542A](https://doi.org/10.1039/B604542A)
- Qin D, Xia Y, Rogers JA, Jackman RJ, Zhao X-M, Whitesides GM (1998) Microfabrication, microstructures and microsystems. In: Manz A, Becker H (eds) *Microsystem Technology in Chemistry and Life Science*. Springer, Berlin, Heidelberg, pp 1–20. doi:[10.1007/3-540-69544-3_1](https://doi.org/10.1007/3-540-69544-3_1)
- Ramadan Q, Samper V, Poenar D, Yu C (2006a) Magnetic-based microfluidic platform for biomolecular separation. *Biomed Microdevices* 8:151–158. doi:[10.1007/s10544-006-7710-x](https://doi.org/10.1007/s10544-006-7710-x)
- Ramadan Q, Samper V, Poenar DP, Yu C (2006b) An integrated microfluidic platform for magnetic microbeads separation and confinement. *Biosens Bioelectron* 21:1693–1702. doi:[10.1016/j.bios.2005.08.006](https://doi.org/10.1016/j.bios.2005.08.006)
- Richards AJ, Roath OS, Smith JS, Watson JHP (1996) The mechanisms of high gradient magnetic separation of human blood and bone marrow. *IEEE Trans Magn* 32:459–470. doi:[10.1109/20.486533](https://doi.org/10.1109/20.486533)
- Roath S, Smith AR, Watson JHP (1990) High-gradient magnetic separation in blood and bone marrow processing. *J Magn Magn Mater* 85:285–289. doi:[10.1016/0304-8853\(90\)90067-Z](https://doi.org/10.1016/0304-8853(90)90067-Z)
- Simonnet C, Groisman A (2005) Two-dimensional hydrodynamic focusing in a simple microfluidic device. *Appl Phys Lett* 87:114104
- Smistrup K, Kjeldsen BG, Reimers JL, Dufva M, Petersen J, Hansen MF (2005) On-chip magnetic bead microarray using hydrodynamic focusing in a passive magnetic separator. *Lab Chip* 5:1315–1319. doi:[10.1039/B510995G](https://doi.org/10.1039/B510995G)
- Song S-H, Lee H-L, Min YH, Jung H-I (2009) Electromagnetic microfluidic cell labeling device using on-chip microelectromagnet and multi-layered channels. *Sensors Actuators B Chem* 141:210–216. doi:[10.1016/j.snb.2009.06.037](https://doi.org/10.1016/j.snb.2009.06.037)
- Tan SJ, Yobas L, Lee GYH, Ong CN, Lim CT (2009) Microdevice for the isolation and enumeration of cancer cells from blood. *Biomed Microdevices* 11:883–892
- Whitesides GM, Kazlauskas RJ, Josephson L (1983) Magnetic separations in biotechnology. *Trends Biotechnol* 1:144–148. doi:[10.1016/0167-7799\(83\)90005-7](https://doi.org/10.1016/0167-7799(83)90005-7)
- Whitesides GM, Ostuni E, Takayama S, Jiang X, Ingber DE (2001) Soft lithography in biology and biochemistry. *Annu Rev Biomed Eng* 3:335–373
- Yellen BB, Erb RM, Son HS, Hewlin JR, Shang H, Lee GU (2007) Traveling wave magnetophoresis for high resolution chip based separations. *Lab Chip* 7:1681–1688. doi:[10.1039/B713547E](https://doi.org/10.1039/B713547E)
- Zborowski M, Sun L, Moore LR, Stephen Williams P, Chalmers JJ (1999) Continuous cell separation using novel magnetic quadrupole flow sorter. *J Magn Magn Mater* 194:224–230. doi:[10.1016/S0304-8853\(98\)00581-2](https://doi.org/10.1016/S0304-8853(98)00581-2)